land

MDPI

Article

Impacts of Land Use Types, Soil Properties, and Topography on Baseflow Recharge and Prediction in an Agricultural Watershed

Chong Wei [1,2], Xiaohua Dong [1,2,*], Yaoming Ma [3,4,5,6,7,8,*], Wenyi Zhao [1,2], Dan Yu [1,2], Muhammad Tayyab [1,2] and Huijuan Bo [1,2]

1 College of Hydraulic & Environmental Engineering, China Three Gorges University, Yichang 443002, China
2 Engineering Research Center for the Ecological Environment of the Three Gorges Reservoir Area, Ministry of Education, Yichang 430072, China
3 Land-Atmosphere Interaction and Its Climatic Effects Group, State Key Laboratory of Tibetan Plateau Earth System, Resources and Environment (TPESRE), Institute of Tibetan Plateau Research, Chinese Academy of Sciences, Beijing 100101, China
4 College of Earth and Planetary Sciences, University of Chinese Academy of Sciences, Beijing 100049, China
5 College of Atmospheric Science, Lanzhou University, Lanzhou 730000, China
6 National Observation and Research Station for Qomolongma Special Atmospheric Processes and Environmental Changes, Shigatse 858200, China
7 Kathmandu Center of Research and Education, Chinese Academy of Sciences, Beijing 100101, China
8 China-Pakistan Joint Research Center on Earth Sciences, Chinese Academy of Sciences, Islamabad 45320, Pakistan
* Correspondence: xhdong@ctgu.edu.cn (X.D.); ymma@itpcas.ac.cn (Y.M.)

Abstract: Baseflow is an essential component of runoff, which is the dominant water resource for the dry season. To better manage water resources, it is vital to investigate the links between the multiple influencing factors and the baseflow for better prediction in light of global changes. Previous studies have seldom separated these influencing factors in the analysis, making it difficult to determine their effect on the baseflow. In this study, based on the analysis datasets generated by the Soil and Water Assessment Tool (SWAT) model, the control single variables, correlation analysis, and multiple linear regression (MRL) methods were firstly combined to analyze the influences of the chosen factors (land use, topography, and soil type) on the baseflow. The findings revealed that the ability of precipitation to replenish the baseflow was better in areas with a higher slope. The ability of precipitation to recharge the baseflow for different land uses was ranked as "forest land > grass land > agricultural land > urban land"; land use factors should be added to the baseflow prediction equation. The hydrological group is the main property of soil affecting the baseflow recharge. A regression model established using publicly acquired remote sensing data had a good performance (R^2 = 0.84) on baseflow prediction on an annual scale. As a result of this information, relevant government officials and environmentalists may better manage water supplies in drought years. In addition, this regression model frame has the potential to be used for a baseflow inquiry inside an ungauged zone for a better ecological assessment.

Keywords: baseflow; land use; soil property; SWAT model; control variable method; MRL analysis

check for updates

Citation: Wei, C.; Dong, X.; Ma, Y.; Zhao, W.; Yu, D.; Tayyab, M.; Bo, H. Impacts of Land Use Types, Soil Properties, and Topography on Baseflow Recharge and Prediction in an Agricultural Watershed. *Land* **2023**, *12*, 109. https://doi.org/10.3390/land12010109

Academic Editor: Guangju Zhao

Received: 28 November 2022
Revised: 20 December 2022
Accepted: 28 December 2022
Published: 29 December 2022

1. Introduction

Water resources are an important component of the ecological environment, which have changed during human development [1–3], further affecting the ecological environment [4,5]. Many types of studies have been conducted to investigate the variation in water resources due to anthropogenic activities and climate change [6–9], for better water resources management, ecological balance and sustainable development. Baseflow is an important portion of water resources, which plays an important role in the dry seasons [10,11],

and is vital for the biosphere [12], ecology [13,14], agriculture [15,16], and human development [17]. It is of great significance to investigate the influencing factors of the baseflow for a better understanding of the baseflow in light of global changes.

The definition of baseflow is controversial. Some scholars regard subsurface return flow and lateral flow as baseflow [18,19], while other researchers only use the subsurface return flow as the baseflow [20]. In addition, the influencing factors of the baseflow are complex, including land use, topography, climate, geology, anthropogenic activities, etc. [10,21–23]. At present, the most used methods in investigating the baseflow change mechanisms are statistical methods, hydrological similarities, and hydrological models [24]; several studies have analyzed the explanation for baseflow changes in many regions from various aspects in recent years. However, the lack of a unified definition and complex influencing factors result in discrepancies in the relevant research results. Previous studies have revealed that land use change is an important influencing factor for baseflow variations. Ahiablame et al. [23] and Ayers et al. [25] found that the baseflow increased with the increase in agricultural land, while Charlier et al. [26] and Huang et al. [27] evidenced that the increases in agricultural land led to a decrease in the baseflow. Most studies have found that forests increase baseflow compared to non-forest regions [28,29]; however, one scholar obtained the inverse results [27]. In addition, some studies have found that urbanization [30], and anthropogenic agricultural activities (i.e., drainage tiling [31] and agricultural management [13]) affect baseflow significantly. Apart from land use, the baseflow response varied with the geomorphic and hydrogeologic settings [32,33], and the precipitation and antecedent wetness affected the baseflow significantly with a different changing trend [34,35]. Most scholars have indicated that baseflow is a complex process affected by the interaction of land use, topography, geology, climate, anthropogenic activities, and other unknown factors [23,34,36]. In general, the change mechanism of baseflow varies in different regions.

To reveal the interaction between these driving factors and baseflow, some scholars have used statistical methods to analyze the relationship between these factors and baseflow [37,38], and some scholars have developed regression models to predict baseflow based on various driving factors [22,35]. However, these studies could not distinguish the influence of different driving factors on the baseflow nor control the variables well. The Soil and Water Assessment Tool (SWAT) model [39] is a physical-based semi-distributed hydrological model, widely used in hydrology investigation [8,40–42] and in baseflow investigation [18,21]. In previous studies relevant to baseflow, the SWAT model was used as a hydrological series generator by simulating the hydrological processes under different scenarios. The SWAT model separates watersheds into several sub-watersheds, which are further divided into Hydrological Response Units (HRUs) based on land use, soil, and slope combination [39]. Benefitting from this simulation mechanism of the SWAT model, it is a good tool to realize the control variables (land use type, slope, and soil properties) to analyze the baseflow response to various driving factors, which could avoid the interaction effect of different driving factors on the baseflow. However, studies using the SWAT model to carry out such analysis based on the control single variable method have not been previously reported.

Baseflow is the guarantee for the balanced development of the watershed's ecology and the most basic source of water resources [14]. It plays an important role, particularly in an agricultural watershed. The Xixian watershed (XXW), located at the source of the Huaihe River Basin, China, is an agricultural watershed, where agricultural land occupies 55% of the total area [43]. Farmers within XXW plant rice, corn, and winter wheat across the whole year, which need water resources for agricultural irrigation. Baseflow is an important water source for local anthropogenic activities and ecological balance, especially during the non-flood season. Understanding the driving factors of baseflow within the watershed is of significant importance for better water resource management. Based on this, XXW was chosen as the study region. The main purposes of this paper are (1) to use correlation analysis and the control single variable method to analyze the baseflow

response with selected driving factors based on the HRU output of the SWAT model; (2) to use multiple linear regression (MLR) to analyze the baseflow response with selected driving factors at the HRUs scale and sub-watershed scale; (3) to combine the results from these two methods and analyze the effects of the chosen driving factors on baseflow, to better predict baseflow.

2. Materials and Methods

2.1. Study Area

Xixian watershed (XXW) is located in the upper area of the Huaihe River Basin in China, with an area of 10,229 km^2, between 112° and 121° E and 31° and 35° N (Figure 1). XXW originates from Tongbai Mountain, with an elevation between 0 (lowest) and 1138 (highest) m upper sea level. The watershed is located in the transition region between the warm temperate zone and the northern subtropical zone [44], with diverse terrain (containing mountains, hills, and flat areas). Within XXW, the annual average temperature is about 11–16 °C, and the average annual precipitation is about 950 mm and varies from 800 to 1000 mm across this area [42]. The rainy season ranges from May to October, with about 60% of the total annual precipitation.

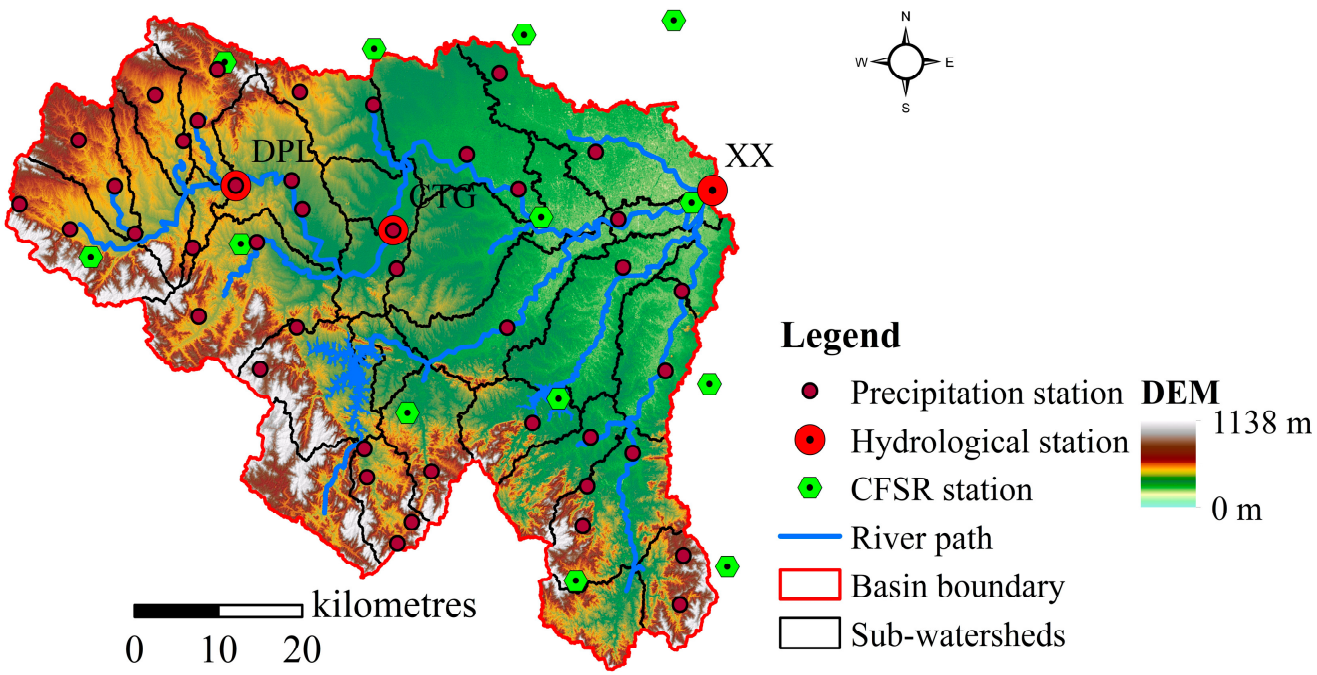

Figure 1. Description of the Xixian watershed. DPL, CTG, and XX represent Dapoling, Changtaiguan, and Xixian hydrological stations, respectively. The CFSR stations are the Climate Forecast System Reanalysis climate stations.

The dominant land use of XXW is agricultural land and forest land, which occupy about 55.3% and 35.9% of the total area, respectively; urban land, water area (containing lakes, rivers, and reservoirs, etc.), and grass land occupy about 4.7%, 3.2%, and 0.9%. The main agricultural patterns are paddy farming and dry farming, across the whole year. A large amount of water is needed for irrigation and to guarantee the production of crops. The uneven precipitation distribution results in the main irrigation water for dry season crops being the baseflow; hence, investigation into the effects of the relevant driving factors on baseflow is needed for agricultural water management, environmental protection, drought prevention, etc.

2.2. Research Approach

To achieve our purposes in this research, our research approaches were as follows and as shown in the workflow in Figure 2:

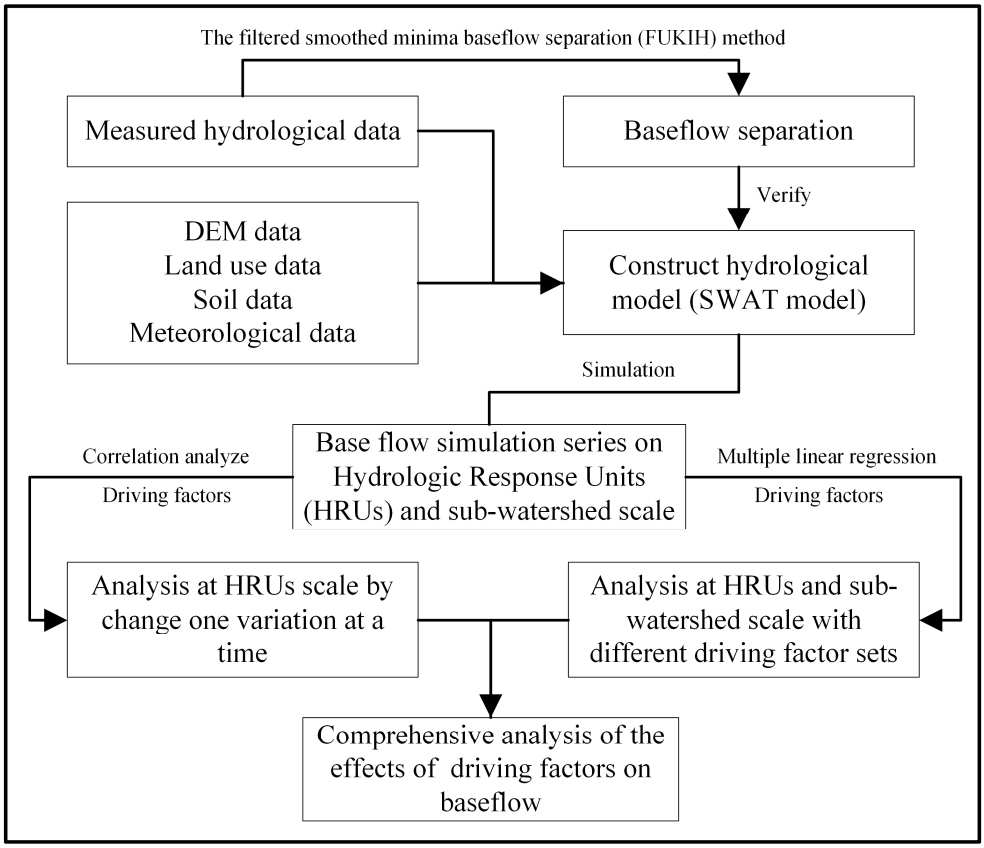

Figure 2. Workflow of the research.

(1) The filtered smoothed minima baseflow separation (FUKIH) method [45] was used to examine the baseflow ratio of the XXW and to guarantee the proportion of baseflow and surface flow was simulated appropriately in the SWAT model. (2) The SWAT model was built to simulate the hydrological process for different underlying surface conditions. (3) Some driving factors were selected to analyze their effects on the baseflow. (4) Two statistical methods (correlation analysis and multiple linear regression) were used to analyze the relationships between the driving factors and baseflow. (5) We compared the results with two statistical methods and found a comprehensive relationship between these driving factors and baseflow, which can better predict baseflow.

2.3. Data Descriptions

XXW was chosen as the study area, data within XXW were used including the digital elevation model (DEM), land use maps, soil maps, weather data, daily precipitation series, and long-term continuous streamflows. The DEM was obtained from the Geospatial Data Cloud (http://www.gscloud.cn, accessed on 5 May 2022), with a resolution of 30 m. The land use map was obtained from the Resource and Environment Science and Data Center (https://www.resdc.cn, accessed on 5 May 2022), its resolution was 30 m, and was separated into five categories: agricultural land, forest land, grass land, water area, and urban land (Figure 3). The soil map published by the Food and Agriculture Organization (Harmonized Word Soil Database v 1.2) was used in this study, with a resolution of 30 arc-second, further resampled into 30 m, to have the same resolution as the DEM and land use map (Figure 3). Weather data during 1979–2013 were downloaded from Climate Forecast System Reanalysis (CFSR, https:

//climatedataguide.ucar.edu/climate-data/climate-forecast-system-reanalysis-cfsr, accessed on 5 March 2020), and 14 stations were selected to calculate the weather generator parameters for the SWAT model, including precipitation, temperature, wind speed, humidity, and solar radiation. Continuous measured daily precipitation series from 1980 to 2012 were obtained from 42 precipitation stations supplied by the Hydrologic Bureau of Huaihe River Commission. The long-term continuous streamflow for three hydrological stations (Streamflow series of XX station were from 1980 to 2012, while DPL and CTG were from 1985 to 2012) were obtained from the Hydrologic Bureau of Huaihe River Commission.

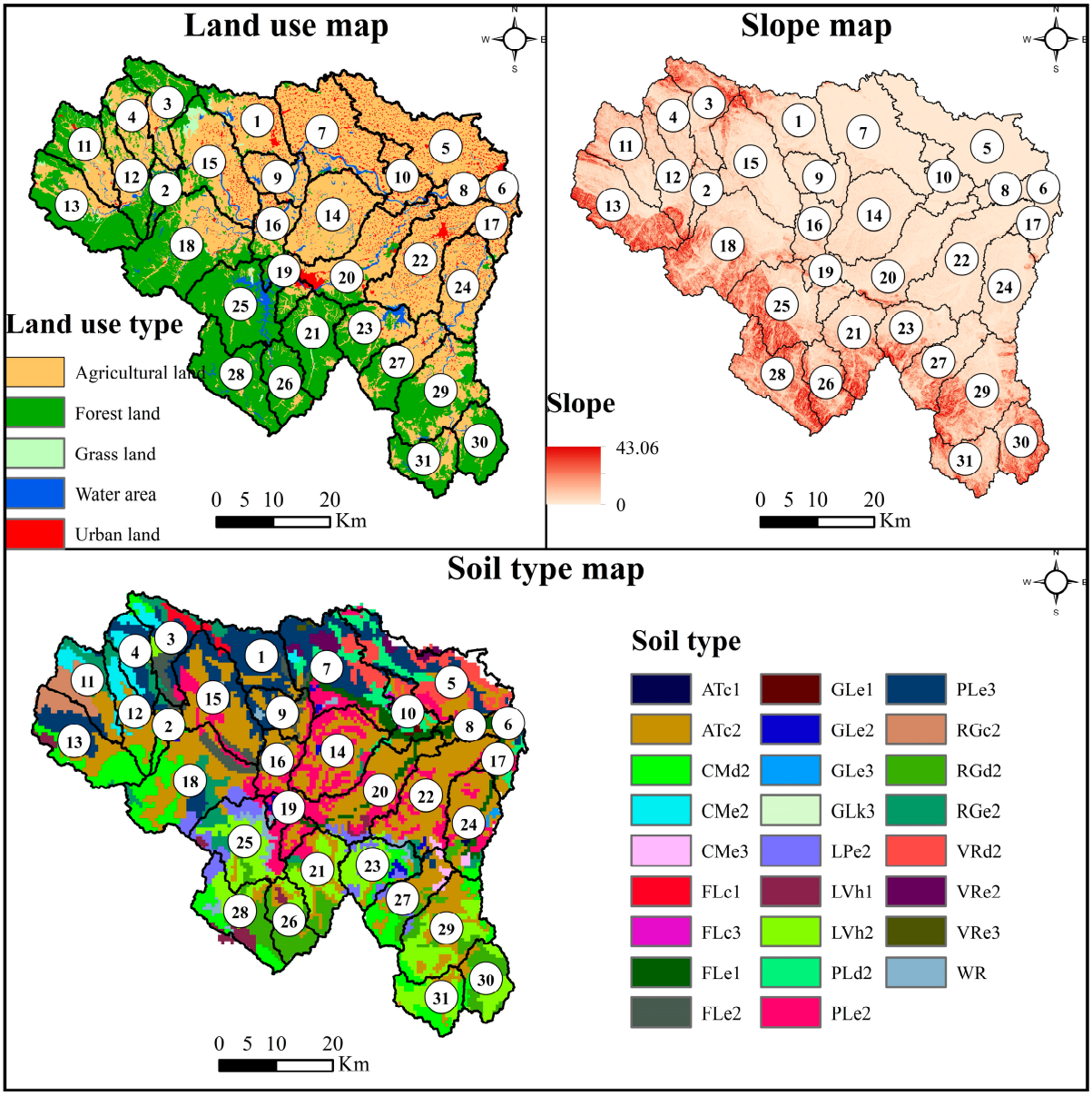

Figure 3. Distribution of land use, slope, and soil type within the XXW. Numbers (1–31) with circles indicate subwatershed numbers. The number after the soil type code indicates the soil texture. "ATc", "CMd", "CMe", "FLc", "Fle", "Gle", "GLk", "LPe", "LVh", "PLd", "PLe", "RGc", "RGd", "RGe", "VRd", "VRe", and "WR" represent cumulic anthrosols, dystric cambisols, eutric cambisols, calcaric fluvisols, eutric fluvisols, eutric gleysols, calcic gleysols, eutric leptosols, haplic luvisols, dystric planosols, eutric planosols, calcaric regosols, dystric regosols, eutric regosols, dystric vertisols, eutric vertisols, and water bodies, respectively.

2.4. Baseflow Separation

Hydrologists have developed a series of separation methods to divide the surface runoff and the baseflow; these methods can be broadly divided into three groups: (1) graphical methods, (2) filtering methods, and (3) mass balance methods [19,38]. The filtered smoothed minima baseflow separation (FUKIH) method [45] combines the advantages of the minimum algorithm and filter algorithm and can separate natural runoff appropriately.

First, the continuous daily runoff is divided by the smooth minimum method for the first time, and then the result of the division is filtered forward by the digital filter method. This method has been applied to many studies and obtains satisfactory results due to its simplicity [46–48]. More details on this method can be found in Aksoy et al. [45]. The definition of the baseflow index (BFI) is the ratio of the baseflow to the total streamflow, which is widely used to describe the characteristic of the baseflow. The BFI of the XXW was 0.3069, which was calculated by continuous daily runoff records from 1980 to 2012 from Xixian hydrological station.

2.5. The SWAT Model

The SWAT model was developed by the Agricultural Research Center of the United States Department of Agriculture (USDA), one of the most widely used semi-distributed hydrological models. The SWAT model divides the watershed into several sub-watersheds based on sub-catchment regions calculated from the DEM and further separates them into HRUs based on land use, soil type, and slope belt. It can directly express the differences in spatial attributes in different sub-watersheds, even in HRUs. Benefitting from these features of the SWAT model, many researchers have adopted it to investigate the hydrological responses to land use and climate change to obtain satisfactory results. The SWAT model was used in this study due to its unique combination of land use, soil type, and average slope in each HRU. More details about the SWAT model can be found in Wei et al. [40].

The XXW was divided into 31 sub-watersheds, and further separated into 911 HRUs. Because the response of the baseflow is not as sensitive as surface flow, the analysis of this study was carried out on a monthly scale. To ensure the simulation results were reasonable in space, the measured streamflow (1987–2012) at three hydrological stations (DPL, CTG, and XX) were used to calibrate and validate the SWAT model. The years of 1985–1986, 1987–2002, and 2003–2012 were chosen as the warm-up period, calibration period, and validation period, respectively.

The SWAT-CUP [49] was chosen as the tool to analyze the sensitivity of the parameters and calibrate the sensitive parameters. We used the one-at-a-time method to evaluate the sensitivity of the parameters, and the SUFI-2 algorithm was used to calibrate the sensitive parameters. The Nash-Sutcliffe coefficient (*NSE*), Percent Bias (*PBIAS*), and the ratio of the root mean square error to the standard deviation (*RSR*) were chosen to evaluate the performance of the SWAT model; further descriptions of these indicators are given in Moriasi et al. [50].

The calibrated SWAT model was performed during 1987–2012, which obtained the baseflow series during this period. The monthly and annual output of the SWAT on the HRUs and subwatershed scale were used in the analysis in Sections 3.2–3.4.

2.6. Driving Factor Selection

The SWAT model was the main tool to obtain the series to carry out the analysis, which separated watersheds into sub-watershed and further divided these into HRUs. Each HRU generated by the SWAT model consisted of a unique combination of land use, soil, and slope within the sub-watershed, and the precipitation in the HRUs was different in different months or years. The Hydrology Group is an index proposed by Staff [51]; the soils were separated into different hydrology groups (A, B, C, and D) based on their infiltration character, and these were used in the SWAT model. The infiltration capability decreased from A to D when the soil reached its full water content. Hence, land use

type, soil type, hydrology group, average slope, area, and precipitation were chosen as the driving factors for baseflow analysis at the HRU scale. For the sub-watershed scale, some land use indicators (the agricultural land area ratio, forest land area ratio, and urban land area ratio) and terrain indicators (average elevation) were added to the previous driving factors. The agricultural land area ratio, forest land area ratio, and urban land area ratio represented the percent of agricultural land, forest land, and urban land within the XXW, respectively.

2.7. Statistical Methods

Correlation analysis is a statistical analysis method that investigates the correlation between two or more random variables in the same position, and it has been widely used in hydrology research [52,53]. The XXW lacks alpine snowmelt; hence, its groundwater is mainly fed by precipitation. Therefore, the effects on the baseflow from other driving factors are mainly reflected by the changes in the relationship between the precipitation and the baseflow. Correlation analysis and linear regression analysis were carried out between the precipitation and baseflow with different combinations of land use, soil type, and slope based on the HRU output to obtain the regression coefficient (RC, the "a" in the equation "Baseflow = a × Precipitation + b" established for each combination mentioned before). The change in the RC represents the changes in the ability of the precipitation to replenish the ground water. In addition, Pearson's correlation coefficient (PCC) was used to evaluate the accuracy of the regression equation for each combination. In this way, we could investigate the impacts of these driving factors on the relationship between precipitation and baseflow; further, we could analyze the effect of these driving factors on baseflow recharge. These analyses based on the correlation analysis and linear regression analysis are conducted in Section 3.2.

Multiple linear regression (MLR) is widely used in investigating the relationship between some factors of the baseflow, many of these investigations established an empirical equation for these factors to predict the baseflow [34,35,37]. On the HRU scale, MLR was performed for the independent variables (average slope, area, and precipitation) and dependent variable (baseflow) with different combinations of land use and soil/hydrology group; while on the sub-watershed scale, MLR was performed for the independent variables (area, agricultural land area ratio, forest land area ratio, urban land area ratio, average slope, average elevation, and precipitation) and the dependent variable (baseflow). The regression formulations are shown in Table 1; the coefficient of determination (R^2) was used to evaluate the accuracy of these formulations. The analyses based on the MLR and the equation formulation in Table 1 are described in Sections 3.3 and 3.4.

Table 1. MLR formulations with different scales.

Driving Factors	Model Formulation	Spatial Scale
Average slope (as), area (ar), precipitation (pr)	Baseflow = a * as + b * ar + c * pr + d	HRUs
Area (ar), agricultural land area ratio (agr), forest land area ratio (flr), urban land area ratio (urr), average slope (as), average elevation (ae), precipitation (pr)	Baseflow = e * ar + f * agr + g * flr + h * urr + I * as + j * ae + k * pr + l	Sub-watershed

Note: "a", "b", "c", "e", "f", "g", "h", "i", "j", and "k" are the regression coefficient for different independent variables in the MRL equation, and "d" and "l" are the constant terms in the MRL equation. The "*" represents multiple sign.

3. Results

3.1. Performance of the Established SWAT Model

The most sensitive parameters within the XXW were the CN2 (initial SCS runoff number for moisture condition II), the ESCO (soil evaporation compensation factor), and

the REVAPMN (threshold depth of the water in the shallow aquifer for "revap" to occur), followed by the EPCO (plant uptake compensation factor), the GW_DELAY (ground water delay), the RCHRG_DP (deep aquifer percolation fraction), the SOL_AWC (available water capacity of the soil layer), the ALPHA_BF (baseflow alpha factor), the SOL_Z (depth from the soil surface to the bottom of the layer), and the CANMX (maximum canopy storage). These 10 sensitive parameters were calibrated, and the performance of the fittest parameter sets was evaluated as shown in Table 2, the measured and simulated runoff values were shown in Figure 4.

Table 2. Evaluation indicators for SWAT model calibration.

Period	Time	Station	NSE	PBIAS	RSR
Calibration	1987–2002	DPL	0.93	−4.5	0.26
		CTG	0.91	−2.0	0.29
		XX	0.88	−6.4	0.34
Validation	2003–2012	DPL	0.92	1.2	0.28
		CTG	0.93	−0.4	0.26
		XX	0.89	−0.5	0.33

Note: The NSE ranges from $-\infty$ to 1 (a better value), the PBIAS ranges from 0 (a better value) to ∞, and the RSR ranges from 0 (a better value) to $+\infty$.

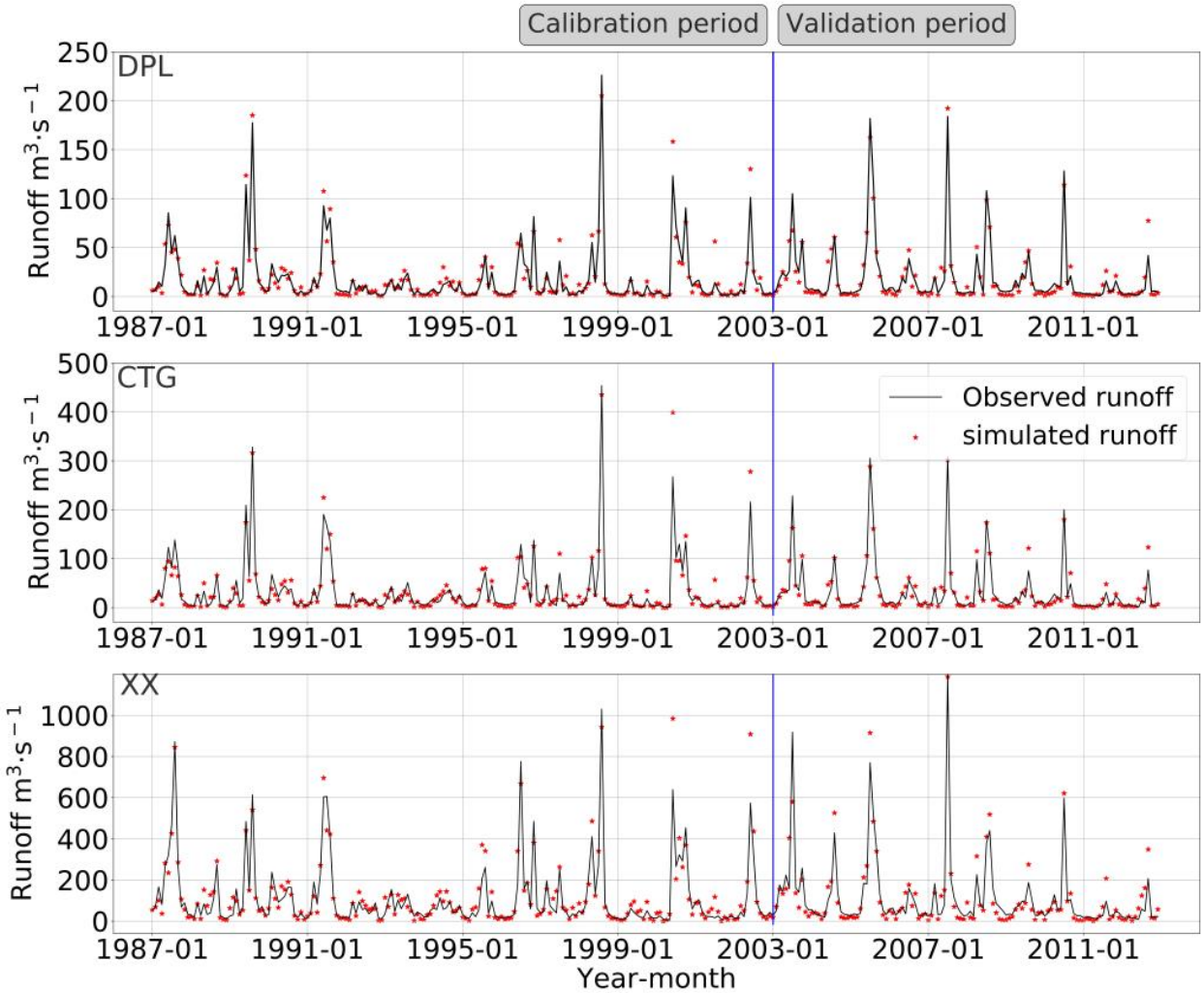

Figure 4. Comparison between the measured and simulated runoff values for the SWAT model in the DPL, CTG, and XX stations.

As seen in Table 2, the *NSE*, *PBIAS*, and *RSR* for all stations ranged from 0.88 to 0.93, −6.4 to 1.2, and 0.26 to 0.34, respectively. As recommended by Moriasi et al. [50], when 0.75 < *NSE* < 1.0, *PBIAS* < ±10, and 0 < *RSR* <0.5 for monthly streamflow, these indicate the SWAT model's performance is very good. As seen in Figure 4, the simulated runoff was consistent with the measured runoff in most months, with several high values overestimated. For most low flow months, the simulated and measured runoff had good consistency, which indicated that the months that were dominated by the baseflow were simulated appropriately. In addition, the parameters were manually adjusted after automatic calibration, so the BFI of the simulation results was consistent with the actual values. Finally, the BFI simulated ((lateral flow + shallow groundwater)/total streamflow) in the SWAT model was 0.3095 for the whole XXW, and the BFI separated from measured streamflow data was 0.3069 by FUKIH. Thus, we concluded that the simulated baseflow was consistent with the actual baseflow, and the simulation results of the SWAT were used in this study.

3.2. Correlation Analysis at HRU Scale

As shown in Figures 5 and 6, the PCC and RC of the precipitation and baseflow were changed with different combinations of land use, soil type, and slope both on a yearly and monthly scale. The range of the PPC of the precipitation and baseflow for agricultural land, forest land, grass land, and urban land was 0.73–0.96, 0.92–0.98, 0.89–0.96, and 0.59–0.94, respectively, on a yearly scale. The range of the PPC of the precipitation and baseflow for agricultural land, forest land, grass land, and urban land was 0.32–0.83, 0.64–0.86, 0.64–0.84, and 0.22–0.81, respectively, on a monthly scale. The range of the RC of the precipitation and baseflow for agricultural land, forest land, grass land, and urban land was 0.09–0.41, 0.27–0.76, 0.19–0.64, and 0.04–0.4, respectively, on a yearly scale. The range of the RC of the precipitation and baseflow for agricultural land, forest land, grass land, and urban land was 0.02–0.3, 0.12–0.51, 0.08–0.46, and 0.01–0.27, respectively, on a monthly scale. These results indicated that the ability to replenish the baseflow was ranked as "forest land > grass land > agricultural land > urban land" for almost all combinations of soil type and slope belt within the XXW. The PPCs on the annual scale were higher than that on the monthly scale, which may be caused by the lag time during the replenishment of the baseflow by precipitation. The results of the RC were similar to that of the PCC, which further supported this conclusion. In addition, the variation ranges in the PCC of the precipitation and baseflow for each land use were smaller for a high slope belt than that for a low and middle slope belt. With the increase in the slope, the PCCs of the precipitation and baseflow were increased for several soil types.

We divided the soil types into three categories based on their hydrology group. As shown in Table 3, the PCC and RC of the precipitation and baseflow all decreased from hydrology A to C. The PPC (RC) of the agricultural land, forest land, grass land, and urban land decreased from 0.796–0.915 (0.266–0.434), 0.826–0.952 (0.462–0.778), 0.822–0.968 (0.367–0.598), and 0.780–0.956 (0.230–0.392) to 0.226–0.664 (0.001–0.009), 0.546–0.850 (0.073–0.180), 0.146–0.760 (0.003–0.022), and 0.239–0.762 (0.001–0.011), respectively. This shows that the replenishing ability of the precipitation on the baseflow decreased when the hydrology group of the soil changed from A to C.

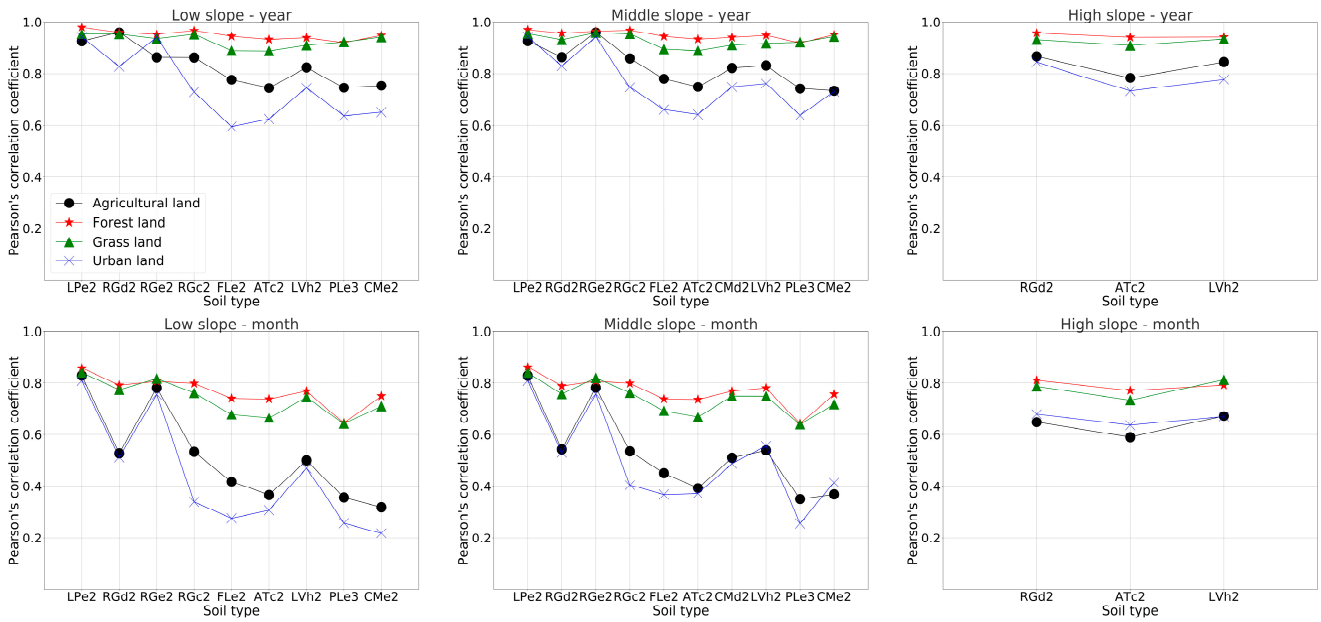

Figure 5. The PCC of the precipitation and baseflow for different combinations of land use, soil type, and slope. The low slope, middle slope, and high slope represented the slope ranges 0–10, 10–25, and 25–40, respectively. "Year" and "month" mean the data of the samples were on a yearly and monthly scale, respectively. The soil type name of each soil type code is defined in Figure 3.

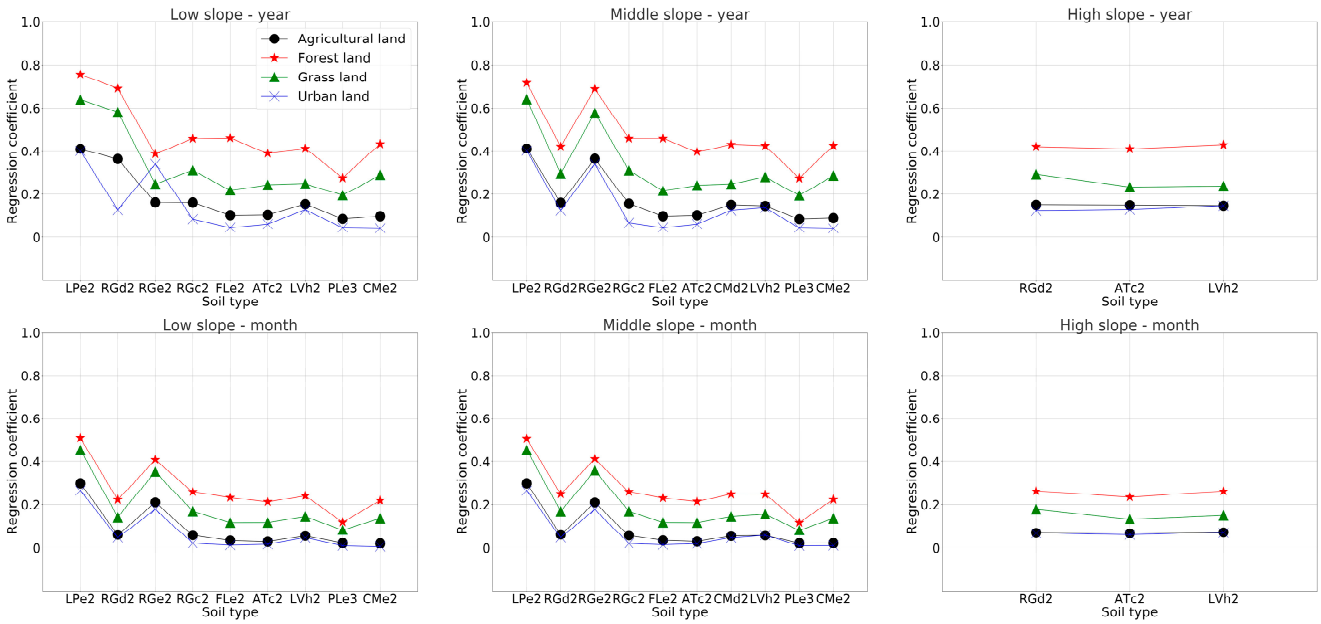

Figure 6. The RC between the precipitation and baseflow for different land uses, soil types, and slopes. The RC is the "a" of the equation "Baseflow = a × Precipitation + b" for each combination of land use, soil/hydrology group, and slope. The low slope, middle slope, and high slope represent the slope ranges 0–10, 10–25, and 25–40, respectively. "Year" and "month" mean the data of the samples were on a yearly and monthly scales, respectively. The soil type name of each soil type code is defined in Figure 3.

Table 3. The PPCs and RC for precipitation and baseflow for different combinations of land use, hydrology group, and slope range. a and b are the coefficient of the equation "Baseflow = a * Precipitation + b" established for each combination of land use, hydrology group, and slope range.

Land Use	Hydrology Group	Slope Range	Yearly			Monthly		
			a (RC)	b	PCC	a (RC)	b	PCC
Agricultural land	A	0–10	0.434	−141.421	0.874	0.266	3.511	0.796
		10–25	0.434	−137.781	0.875	0.270	3.407	0.805
		25–40	0.416	−55.293	0.915	0.318	6.007	0.868
	B	0–10	0.125	−78.288	0.775	0.038	0.734	0.422
		10–25	0.122	−71.327	0.773	0.039	1.026	0.445
		25–40	0.143	−54.456	0.836	0.072	2.185	0.650
	C	0–10	0.004	−1.067	0.574	0.001	0.162	0.226
		10–25	0.009	0.522	0.664	0.004	0.388	0.584
		25–40	-	-	-	-	-	-
Forest land	A	0–10	0.778	−372.645	0.952	0.462	−4.526	0.826
		10–25	0.739	−322.630	0.939	0.468	−4.299	0.835
		25–40	0.733	−306.760	0.938	0.489	−5.269	0.855
		40+	0.676	−207.193	0.939	0.514	−3.172	0.877
	B	0–10	0.391	−188.497	0.913	0.214	−1.057	0.738
		10–25	0.408	−197.325	0.920	0.223	−0.770	0.745
		25–40	0.415	−186.592	0.925	0.243	−0.638	0.781
		40+	0.407	−163.330	0.921	0.255	−0.059	0.804
	C	0–10	0.180	−105.720	0.850	0.074	−0.100	0.548
		10–25	0.177	−100.679	0.847	0.073	0.221	0.546
		25–40	-	-	-	-	-	-
Grass land	A	0–10	0.585	−231.359	0.946	0.367	−2.961	0.822
		10–25	0.575	−223.634	0.948	0.372	−2.908	0.829
		25–40	0.568	−203.355	0.943	0.391	−3.241	0.853
		40+	0.598	−256.778	0.968	0.383	−3.820	0.830
	B	0–10	0.240	−122.548	0.876	0.122	−0.821	0.681
		10–25	0.257	−130.583	0.882	0.129	−0.424	0.691
		25–40	0.254	−111.104	0.875	0.139	0.206	0.731
		40+	0.250	−77.114	0.882	0.161	1.621	0.786
	C	0–10	0.022	−9.971	0.502	0.003	0.536	0.146
		10–25	0.021	−8.002	0.515	0.003	0.677	0.153
		25–40	0.021	−3.114	0.760	0.004	0.942	0.245
Urban land	A	0–10	0.390	−172.609	0.913	0.230	−0.444	0.780
		10–25	0.390	−167.537	0.913	0.237	−0.678	0.798
		25–40	0.392	−134.221	0.956	0.300	−1.194	0.918
	B	0–10	0.081	−54.042	0.666	0.024	0.169	0.359
		10–25	0.080	−48.492	0.674	0.026	0.417	0.403
		25–40	0.118	−50.774	0.798	0.063	0.957	0.681
	C	0–10	0.005	−1.657	0.624	0.001	0.194	0.239
		10–25	0.011	−0.063	0.762	0.005	0.406	0.637
		25–40	-	-	-	-	-	-

Among all combinations of land use and hydrology group, in most cases, the PCC and RC of the precipitation and baseflow increased with the increase in the slope, especially for hydrology group C. For example, for the combination of agricultural land and soil with hydrology group C, the RC (PCC) increased from 0.226 to 0.584 on the monthly scale. This indicates that the replenishing ability of the precipitation on the baseflow increased with the increase in slope.

In addition, the increase in the PCC of the precipitation and baseflow was more significant for agricultural land and urban land compared to forest land and grass land. This may indicate that the replenishing ability of the precipitation on the baseflow would be more easier affected by the hydrology group and slope when the land use is agricultural land and urban land, compared to that of forest land and grass land.

3.3. MLR Analysis at the HRU Scale

The MLR was performed for different combinations of land use and soil type, according to the formulation shown in Table 1 on a monthly and yearly scale, and the results are shown in Figures 7 and 8. On the yearly scale, the range of the R^2 of each MLR formulation for agricultural land, forest land, grass land, and urban land was 0.56–0.92, 0.85–0.94, 0.81–0.92, and 0.41–0.88, respectively. On the monthly scale, the range of the R^2 of each MLR formulation for agricultural land, forest land, grass land, and urban land was 0.13–0.69, 0.42–0.75, 0.42–0.7, and 0.07–0.65, respectively. The R^2 for different land use was ranked as "forest land > grass land > agricultural land > urban land" for most soil types.

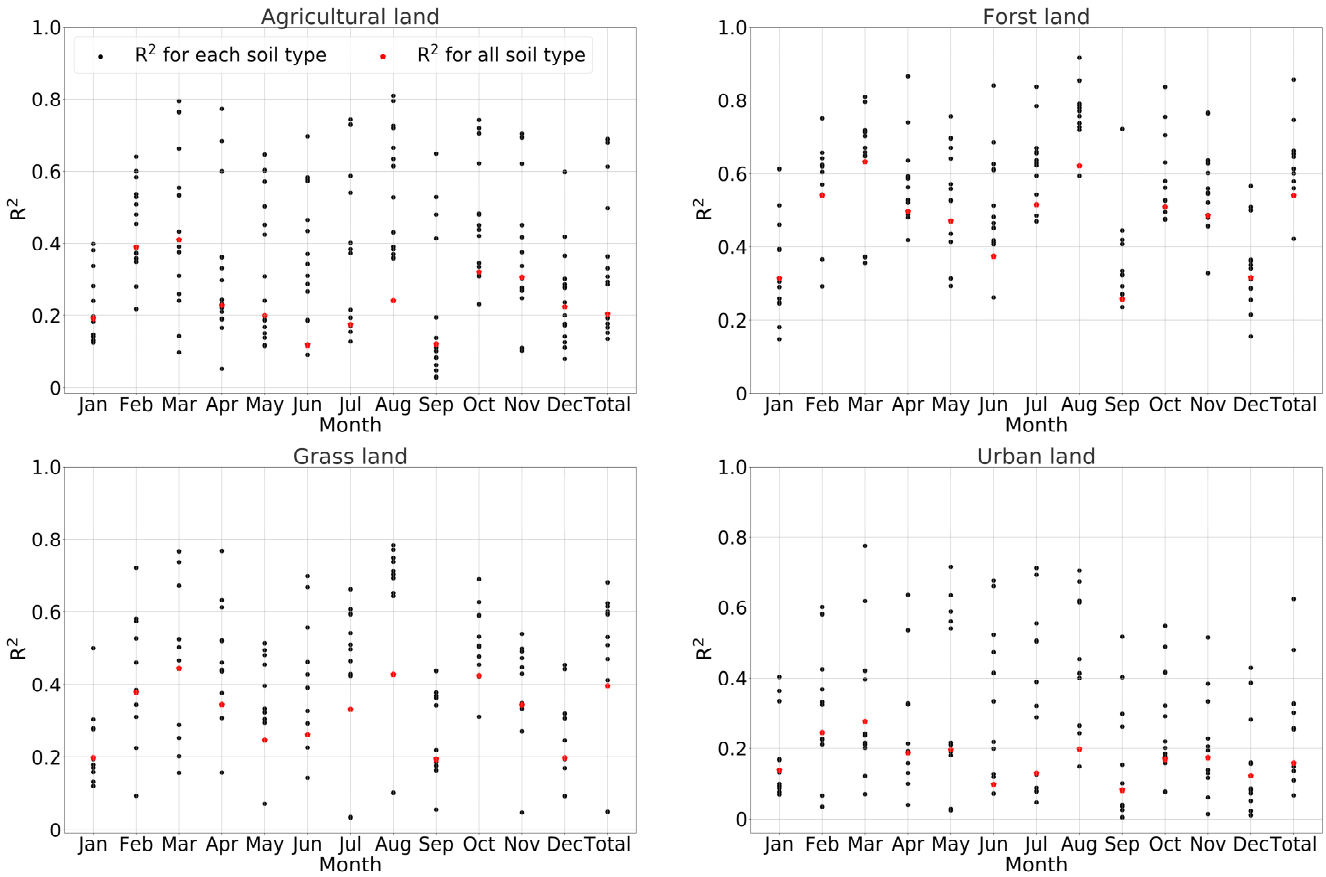

Figure 7. The R^2 of each MLR formulation for different combinations of land use and soil type in different months. The form of the formulation was shown in Table 1. The R^2 for each soil type was the R^2 of the MLR formulation for the HRUs with each different soil type and specific land use type. The R^2 for all soil types was the R^2 of the MLR formulation for the HRUs with all the different soil types and specific land use types. For example, in the first subfigure, the different black points represent the R^2 of the MLR equation established based on the data in the HRUs with a single soil type and agricultural land; while the red points represent the R^2 of the MLR equation established based on the data in the HRUs with all soil type and agricultural land.

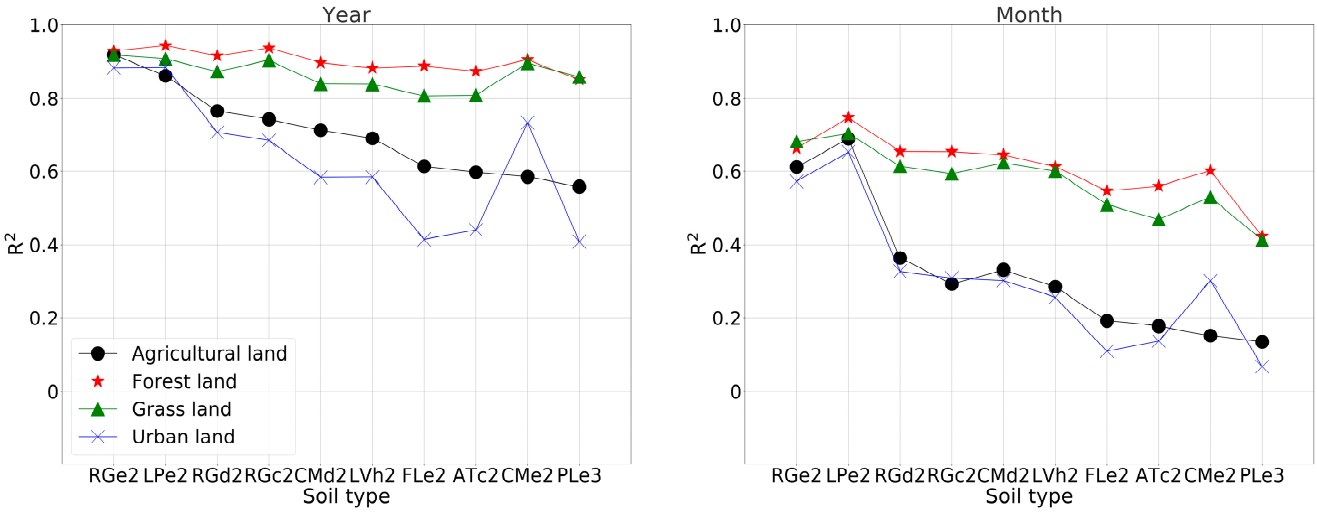

Figure 8. The R^2 of each MLR formulation for different combinations of land use and soil type. The form of the formulation is shown in Table 1. The soil type name of each soil type code refers to Figure 3.

The effect of the soil type on the R^2 of the MLR equation for the forest and grass land was less than that of agricultural and urban land. The R^2 of the MLR equation was higher on the annual scale compared to that on the monthly scale, but the changing trend of the R^2 was similar on an annual and monthly scale. Overall, these differences in the R^2 of the MLR equation for different land use for different soils showed that the soil type could affect the relationship between the precipitation and baseflow.

In different months, the variation of the R^2 was obvious for different soil types for all land uses. The R^2 of the MLR formulation, established by the mixed datasets was lower than that for most of the MLR formulations established by the datasets for each single soil type. For almost all land uses, the R^2 was higher in February, March, August, and October, while it was lower in January, September, and December. This may indicate that the effect of soil type on the baseflow varied in different months, which may result from the growth of different land covers.

The MLR analysis was also performed for different combinations of land use and hydrology group, and the results are shown in Table 4, The R^2 for all land uses decreased from hydrology A to C on the yearly scale. As for the monthly scale, the R^2 for agricultural land and urban land retained the trend of the yearly scale; however, for the R^2 for the agricultural land and urban land, the rank for the different hydrology groups was "A > C > B". The R^2 for hydrology group A was much higher than other hydrology groups, with the ranges 0.85–0.9 and 0.65–0.72 for all land use on a monthly and yearly scale, respectively. These results further show that the effect of the hydrology group on the baseflow exists, and the relationship between the driving factor and the baseflow was more easier established when the hydrology group was A.

Table 4. The R^2 of each formulation for different combinations of land use and hydrology groups.

Land Use	Hydrology Group	R^2	
		Yearly	Monthly
Agricultural land	A	0.792	0.658
	B	0.651	0.239
	C	0.608	0.345
Forest land	A	0.888	0.716
	B	0.854	0.585
	C	0.722	0.300
Grass land	A	0.905	0.702
	B	0.803	0.510
	C	0.328	0.038
Urban land	A	0.846	0.646
	B	0.510	0.187
	C	0.700	0.371

3.4. MRL Analysis at the Sub-Watershed Scale

As shown in Table 5, the R^2 of the MLR formulation at the sub-watershed scale was higher than that at the HRU scale. The agricultural land area ratio, forest land area ratio, urban land area ratio, and average elevation were added into the independent variables to establish the MLR formulation at the sub-watershed scale, which expressed the land use and topography characteristics within the regions. On the yearly scale, the R^2 of the MLR formulation at the sub-watershed and HRU scales were 0.84 and 0.32, respectively; on the monthly scale, the R^2 of the MLR formulation at the sub-watershed and HRU scales were 0.52 and 0.27, respectively. As seen in Figure 9, the R^2 of the MLR formulation at the sub-watershed was higher than that at the HRU scale almost in all months. The range of the R^2 of the monthly MLR formulation at the sub-watershed and HRU scales was 0.32–0.7, and 0.18–0.44, respectively.

Table 5. MLR formulation for different spatiotemporal scales and the R^2 of these formulations. The monthly results were analyzed based on all months; the meaning of the variables is defined in Table 1.

Scale	Time Scale	MLR Formulation	R^2
HRUs	Year	Baseflow = 4.19 * sl + 0.19 * ar + 0.23 * pr−176.76	0.32
	Month	Baseflow = 0.37 * sl + 0.02 * ar + 0.13 * pr−6.09	0.27
Sub-watershed	Year	Baseflow = −0.03 * ar−665.61 * agr−526.59 * flr−721.55 * urr + 6.35 * as−0.2 * ae + 0.22 * pr + 429.98	0.84
	Month	Baseflow = −0.001 * ar−65.22 * agr−53.57 * flr−69.82 * urr + 0.67 * as−0.02 * ae + 0.13 * pr + 49.65	0.52

Note: The "*" represents multiple sign.

These results indicate that land use and elevation are important factors affecting the baseflow. In the MLR formulation on the sub-watershed scale, the driving factors relevant to land use and elevation were taken into consideration compared to that on the HRU scale. In this case, the performance of the MLR formulation improved obviously both on the annual and monthly scale. It is useful to consider the land use component and elevation when establishing a baseflow prediction model, which proved to have an obvious effect on the baseflow recharge.

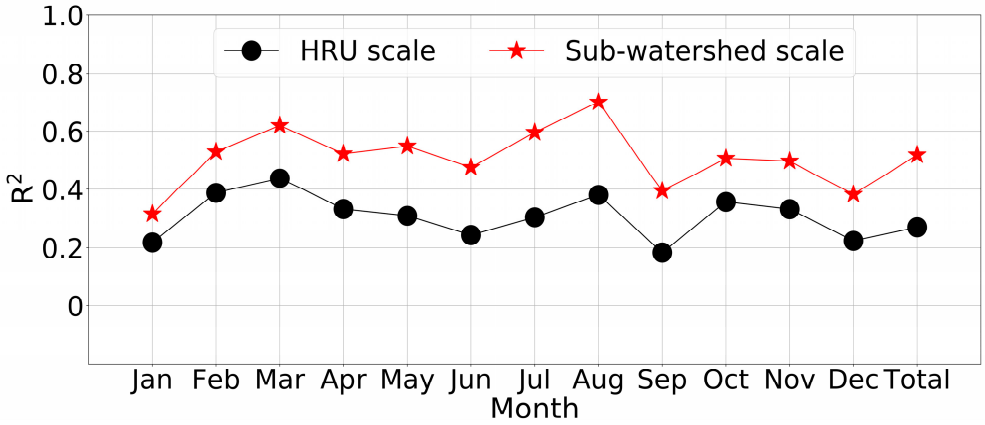

Figure 9. The R^2 of the MLR formulation for different months at HRUs and sub-watershed scales.

4. Discussion

4.1. Impacts of Land Use Type, Soil Type, and Slope on the Baseflow

In our study, the chosen factors were each changed in turn to investigate their influence on the baseflow, based on the various scale outputs of the SWAT model. By the controlling variables method, we found that the PCC and RC of the precipitation and baseflow were different for different land use, soil type, and slope (and). From Table 3, we found that the PCC and RC of the precipitation and baseflow for different hydrology groups were different. The supplemental ability of the precipitation on the baseflow for different land uses ranks as "forest land > grass land > agricultural land > urban land". These results indicated that these factors (land use type, soil type, and slope) change the supplementation of the precipitation to the baseflow. Some studies have also shown that when forest land was converted into other land use types, the baseflow decreased [54,55], and afforestation increased the baseflow [28]. Price [30] indicated that the baseflow decreased under urban land due to the increase in the impervious surface coverage. These findings coincide with ours.

Apart from the land use type, the supplementation ability of the precipitation on the baseflow was changed obviously for different soil types, and these changes had a similar trend to that for different hydrology groups. The soil types that belonged to the same hydrology group, had a similar infiltration capacity when the soil state was completely wet [51]. This result indicates that the infiltration capacity is an important factor for the soil's effect on the recharge of the baseflow. In some theoretical research, the results revealed that intensive soil compaction and an increase in the impervious surface would decrease the infiltration rate and ground water storage recharge, further decreasing the baseflow [56,57]. It is essential to further investigate the effect of soil properties on baseflow by physical experiments.

From Table 3 and Figures 5 and 6, we found that the PCCs and RCs between the precipitation and baseflow on the yearly scale were all better than that on the monthly scale, especially for hydrology B and C. This phenomenon may indicate that the recharge function of the precipitation on the baseflow has a lag time. The PCC was decreased when the land use, soil type, and slope changed, which may indicate that these factors could change the lag time of the recharge function of precipitation on the baseflow. Muñoz-Villers et al. [22] found that the average slope and the infiltration at the soil–bedrock interface were the main factors that influenced the lag time of the baseflow. Some studies denoted that the lag time of the baseflow varied in different locations, ranging from tens of days to more than a year [58–60]. In our study area, according to the high PCCs between precipitation and baseflow on the yearly scale, the lag time of the baseflow was mostly within a year and might differ for the different underlying surfaces. This hypothesis needs to be verified in future studies.

4.2. Baseflow Predicts Regression Model

In previous studies, scholars used agricultural intensity, slope, and meteorological factors (i.e., precipitation, antecedent wetness, and temperature) to predict the baseflow [34,35], further investigating the change mechanism of the baseflow when these factors changed [37,61]. They ignored the soil properties and other land use factors in their baseflow prediction model. In our correlation analysis results, the PCCs between the precipitation and baseflow changed obviously for different land uses and soil types, which indicated that these could significantly affect the baseflow in the watershed.

The MLR analysis was performed for different combinations of land use and soil type on monthly and yearly scales (Figure 8). The performance of the MLR equation for different land uses ranks as "forest land > grass land > agricultural land > urban land" for most cases. These findings may indicate that it is possible to improve the baseflow prediction capacity by adding some driving factors relevant to land use. The results obtained from Figure 7 also indicate that the soil type affected the performance of the MLR equation significantly, the performance of the MLR for all soil types was lower than most MLRs for a single soil type. This also further proves that the baseflow mechanism is different for the different underlying surfaces.

On the sub-watershed scale, some land use factors (agricultural land area ratio, forest land area ratio, and urban land area ratio) and average elevation were added into the independent variables, and MLR analysis was performed with the baseflow as the dependent variable. The R^2 of the MLR equation was 0.84 and 0.52 for the yearly scale and monthly scale, respectively; which was higher than that on the HRU scale (a value of 0.32 and 0.27 for R^2 on the yearly and monthly scale, respectively). The results indicate that the land use factors and elevation are important for baseflow prediction. The mean R^2 for the statistical model in the U.S. Midwest was 0.49 on the monthly scale according to Ayers et al. [34], and the performance of our MLR equation on the sub-watershed (R^2 = 0.52) scale was higher than the mean performance level of the previous study. Zhang et al. [35] used the regression approach to predict the BFI in the long term, adding more land use factors may improve the performance of the prediction model. Apart from the factors chosen in this study, some meteorological and climate factors might also have an important effect on baseflow prediction, which have been mentioned in other research [62–64]. In the future, a series of comprehensive prediction models could be established for baseflow considering all aspects of the influence factors in different climate zones, for better water resource prediction and water management.

4.3. Uncertainties, Deficiency, and Potential Applications

Hydrological modeling has been used to analyze the impact of different factors on hydrology processes [24,27,35], especially distributed hydrological models, which simulated hydrology processes based on physical mechanisms. In this study, the SWAT model was adopted as a tool to investigate the relationships between the chosen factors and the baseflow. Though the SWAT model built in this study had a good performance on runoff and a suitable BFI compared to the actual situation, as stated by Moriasi et al. [50], there still exist some errors introduced by the original data, model mechanism, and equifinality for different parameters [65,66]. However, it is also a suitable tool to investigate the effects of the driving factors on the hydrological components and has been widely used in previous research [18,35,67].

The land use, soil type, and slope were all identified as key factors that influence baseflow, however, there still exist some deficiencies in our results. The number of soil types taken into consideration was low, the slope was separated into four categories, and the results were obtained in a single watershed. More soil types and watersheds need to be taken into consideration in the future, to obtain the universal relationship between these factors and baseflow for most regions. In addition, a smaller slope interval should be used to investigate the relationship between slope and baseflow. Finally, the methods adopted in this study to analyze the effect of the different driving factors on baseflow were

correlation analysis, linear regression analysis, and MLR analysis, which only reveal the linear relationship between several variables. However, these driving factors and baseflow may have a nonlinear relationship; hence, nonlinear regression analysis methods should be applied to address this hypothesis.

Our results indicate that it is better to consider more land use factors when establishing the baseflow prediction equation. In our study, the MLR equation fitting on the sub-watershed had good performance on the yearly scale, with an R^2 of 0.84. The baseflow is the main water resource within the watershed in drought years [68], and the watershed would risk a drought if the precipitation and baseflow were lacking at the same time [57]. It is meaningful to predict the baseflow accurately on a yearly scale, in order to be better prepared for the lack of water for water resource management. The driving factors of this study (area, agricultural land area ratio, forest land area ratio, urban land area ratio, average slope, average elevation, and precipitation) were obtained from remote sensing data. This is a good way to measure the baseflow in an ungauged area, for obtaining a universal equation for different climate zones. For example, the target of this study, XXW, is an agricultural watershed. The MLR equation established at the sub-watershed scale performed well in the baseflow simulation and is beneficial in understanding the condition of the local baseflow. It is significant for local water management in a drought year. In addition, this study has revealed that the land use component has an obvious impacts on baseflow, and in this case, the local government could adjust the land use structure based on these results for better water conservation.

5. Conclusions

The SWAT model established in XXW performed well in the streamflow simulation and could simulate the proper proportion of baseflow. The correlation analysis and MLR analysis were performed to analyze the effects of land use, soil type, and slope on the baseflow. In our results, the PCC between the precipitation and baseflow changed obviously for different combinations of land use, soil type, and slope, and the selected factors all affected the baseflow significantly. The infiltration ability was a key property of soil that affected the baseflow, the PCC between the precipitation and baseflow ranked as "A > B > C" for most conditions. The PCC between the precipitation and baseflow was higher on the yearly scale than that on the monthly scale, which was caused by the lag time effect of the precipitation on the baseflow. The PCC between the precipitation and the R^2 for the MLR equation for different land use was ranked as "forest land > grass land > agricultural land > urban land", and land use is an important factor for the recharge process of baseflow. The performance of the MLR equation established on the sub-watershed scale was better than that on the HRU scale, showing that adding land use factors is a good way to improve the performance of the MLR equation in baseflow prediction. In our study, the independent variables of the MLR equation established at the sub-watershed scale on the yearly scale were all obtained from the remote sensing data and have a good performance (R^2 = 0.84) in baseflow prediction on a yearly scale. It is meaningful for understanding the situation of baseflow, and for better local water management in a drought year.

Author Contributions: Conceptualization, C.W.; Data curation, Y.M. and H.B.; Formal analysis, X.D., W.Z., D.Y. and M.T.; Funding acquisition, X.D., Y.M. and D.Y.; Investigation, C.W., W.Z. and H.B.; Methodology, C.W.; Software, D.Y.; Supervision, X.D. and Y.M.; Visualization, C.W.; Writing—original draft, C.W.; Writing—review and editing, X.D., Y.M. and M.T. All authors have read and agreed to the published version of the manuscript.

Funding: This research has been supported by the Second Tibetan Plateau Scientific Expedition and Research Program (STEP, Grant No. 2019QZKK0103), the European Space Agency (ESA) and National Remote Sensing Center of China (58516), the National Natural Science Foundation of China (No. 52109058), the 2020 Opening fund from Hubei Key Laboratory of Intelligent Vision Based Monitoring for Hydroelectric Engineering (2020SDSJ03), the Construction fund for Hubei Key Laboratory of Intelligent Vision Based Monitoring for Hydroelectric Engineering (2019ZYYD007), the Research

Fund for Excellent Dissertation of China Three Gorges University (No. 2021BSPY002), and the Science and Technology Research Project of Hubei Provincial Department of Education (Q20221209).

Data Availability Statement: Not applicable.

Conflicts of Interest: The authors declare no conflict of interest.

References

1. Altenburger, R.; Ait-Aissa, S.; Antczak, P.; Backhaus, T.; Barceló, D.; Seiler, T.-B.; Brion, F.; Busch, W.; Chipman, K.; de Alda, M.L. Future water quality monitoring—Adapting tools to deal with mixtures of pollutants in water resource management. *Sci. Total Environ.* **2015**, *512*, 540–551. [CrossRef]
2. Brown, K.; Westaway, E. Agency, capacity, and resilience to environmental change: Lessons from human development, well-being, and disasters. *Annu. Rev. Environ. Resour.* **2011**, *36*, 321–342. [CrossRef]
3. Griggs, D.; Stafford-Smith, M.; Gaffney, O.; Rockström, J.; Öhman, M.C.; Shyamsundar, P.; Steffen, W.; Glaser, G.; Kanie, N.; Noble, I. Sustainable development goals for people and planet. *Nature* **2013**, *495*, 305–307. [CrossRef] [PubMed]
4. Liu, J.; Diamond, J. China's environment in a globalizing world. *Nature* **2005**, *435*, 1179–1186. [CrossRef]
5. Zhang, J.; Zhang, C.; Shi, W.; Fu, Y. Quantitative evaluation and optimized utilization of water resources-water environment carrying capacity based on nature-based solutions. *J. Hydrol.* **2019**, *568*, 96–107. [CrossRef]
6. Baker, T.J.; Miller, S.N. Using the Soil and Water Assessment Tool (SWAT) to assess land use impact on water resources in an East African watershed. *J. Hydrol.* **2013**, *486*, 100–111. [CrossRef]
7. Costa, M.H.; Botta, A.; Cardille, J.A. Effects of large-scale changes in land cover on the discharge of the Tocantins River, Southeastern Amazonia. *J. Hydrol.* **2003**, *283*, 206–217. [CrossRef]
8. Gashaw, T.; Tulu, T.; Argaw, M.; Worqlul, A.W. Modeling the hydrological impacts of land use/land cover changes in the Andassa watershed, Blue Nile Basin, Ethiopia. *Sci. Total Environ.* **2018**, *619*, 1394. [CrossRef] [PubMed]
9. Trang, N.T.T.; Shrestha, S.; Shrestha, M.; Datta, A.; Kawasaki, A. Evaluating the impacts of climate and land-use change on the hydrology and nutrient yield in a transboundary river basin: A case study in the 3S River Basin (Sekong, Sesan, and Srepok). *Sci. Total Environ.* **2017**, *576*, 586–598. [CrossRef]
10. Somers, L.D.; McKenzie, J.M.; Zipper, S.C.; Mark, B.G.; Lagos, P.; Baraer, M. Does hillslope trenching enhance groundwater recharge and baseflow in the Peruvian Andes? *Hydrol. Process.* **2018**, *32*, 318–331. [CrossRef]
11. Smerdon, B.D.; Gardner, W.P.; Harrington, G.A.; Tickell, S.J. Identifying the contribution of regional groundwater to the baseflow of a tropical river (Daly River, Australia). *J. Hydrol.* **2012**, *464*, 107–115. [CrossRef]
12. Zhang, J.; Zhang, Y.; Song, J.; Cheng, L.; Gan, R.; Shi, X.; Luo, Z.; Zhao, P. Comparing hydrological modelling, linear and multilevel regression approaches for predicting baseflow index for 596 catchments across Australia. *Hydrol. Earth Syst. Sci. Discuss.* **2017**, 1–40. [CrossRef]
13. Shore, M.; Murphy, S.; Mellander, P.-E.; Shortle, G.; Melland, A.R.; Crockford, L.; O'Flaherty, V.; Williams, L.; Morgan, G.; Jordan, P. Influence of stormflow and baseflow phosphorus pressures on stream ecology in agricultural catchments. *Sci. Total Environ.* **2017**, *590*, 469–483. [CrossRef] [PubMed]
14. Cheng, B.; Li, H.; Yue, S.; Huang, K. A conceptual decision-making for the ecological base flow of rivers considering the economic value of ecosystem services of rivers in water shortage area of Northwest China. *J. Hydrol.* **2019**, *578*, 124126. [CrossRef]
15. Huang, Z.; Ouyang, Z.; Li, F.; Zheng, H.; Wang, X. Response of runoff and soil loss to reforestation and rainfall type in red soil region of southern China. *J. Environ. Sci.* **2010**, *22*, 1765–1773. [CrossRef]
16. Richards, G.; Gilmore, T.E.; Mittelstet, A.R.; Messer, T.L.; Snow, D.D. Baseflow nitrate dynamics within nested watersheds of an agricultural stream in Nebraska, USA. *Agric. Ecosyst. Environ.* **2021**, *308*, 107223. [CrossRef]
17. Kourakos, G.; Dahlke, H.E.; Harter, T. Increasing groundwater availability and seasonal base flow through agricultural managed aquifer recharge in an irrigated basin. *Water Resour. Res.* **2019**, *55*, 7464–7492. [CrossRef]
18. Luo, Y.; Arnold, J.; Allen, P.; Chen, X. Baseflow simulation using SWAT model in an inland river basin in Tianshan Mountains, Northwest China. *Hydrol. Earth Syst. Sci.* **2012**, *16*, 1259–1267. [CrossRef]
19. Yang, W.; Xiao, C.; Zhang, Z.; Liang, X. Can the two-parameter recursive digital filter baseflow separation method really be calibrated by the conductivity mass balance method? *Hydrol. Earth Syst. Sci.* **2021**, *25*, 1747–1760. [CrossRef]
20. Tan, H.; Chen, X.; Shi, D.; Rao, W.; Liu, J.; Liu, J.; Eastoe, C.J.; Wang, J. Base flow in the Yarlungzangbo River, Tibet, maintained by the isotopically-depleted precipitation and groundwater discharge. *Sci. Total Environ.* **2021**, *759*, 143510. [CrossRef]
21. Wang, G.; Yang, H.; Wang, L.; Xu, Z.; Xue, B. Using the SWAT model to assess impacts of land use changes on runoff generation in headwaters. *Hydrol. Process.* **2014**, *28*, 1032–1042. [CrossRef]
22. Muñoz-Villers, L.E.; Geissert, D.R.; Holwerda, F.; McDonnell, J.J. Factors influencing stream baseflow transit times in tropical montane watersheds. *Hydrol. Earth Syst. Sci.* **2016**, *20*, 1621–1635. [CrossRef]
23. Ahiablame, L.; Sheshukov, A.Y.; Rahmani, V.; Moriasi, D. Annual baseflow variations as influenced by climate variability and agricultural land use change in the Missouri River Basin. *J. Hydrol.* **2017**, *551*, 188–202. [CrossRef]
24. Dey, P.; Mishra, A. Separating the impacts of climate change and human activities on streamflow: A review of methodologies and critical assumptions. *J. Hydrol.* **2017**, *548*, 278–290. [CrossRef]

25. Ayers, J.R.; Villarini, G.; Jones, C.; Schilling, K. Changes in monthly baseflow across the US Midwest. *Hydrol. Process.* **2019**, *33*, 748–758. [CrossRef]
26. Charlier, J.B.; Cattan, P.; Moussa, R.; Voltz, M. Hydrological behaviour and modelling of a volcanic tropical cultivated catchment. *Hydrol. Process. Int. J.* **2008**, *22*, 4355–4370. [CrossRef]
27. Huang, X.-D.; Shi, Z.-H.; Fang, N.-F.; Li, X. Influences of land use change on baseflow in mountainous watersheds. *Forests* **2016**, *7*, 16. [CrossRef]
28. Ma, X.; Xu, J.; Luo, Y.; Prasad Aggarwal, S.; Li, J. Response of hydrological processes to land-cover and climate changes in Kejie watershed, south-west China. *Hydrol. Process.* **2009**, *23*, 1179–1191. [CrossRef]
29. Tarigan, S.; Wiegand, K.; Slamet, B. Minimum forest cover required for sustainable water flow regulation of a watershed: A case study in Jambi Province, Indonesia. *Hydrol. Earth Syst. Sci.* **2018**, *22*, 581–594. [CrossRef]
30. Price, K. Effects of watershed topography, soils, land use, and climate on baseflow hydrology in humid regions: A review. *Prog. Phys. Geogr.* **2011**, *35*, 465–492. [CrossRef]
31. Schilling, K.E.; Gassman, P.W.; Arenas-Amado, A.; Jones, C.S.; Arnold, J. Quantifying the contribution of tile drainage to basin-scale water yield using analytical and numerical models. *Sci. Total Environ.* **2019**, *657*, 297–309. [CrossRef] [PubMed]
32. Wang, T.; Istanbulluoglu, E.; Lenters, J.; Scott, D. On the role of groundwater and soil texture in the regional water balance: An investigation of the Nebraska Sand Hills, USA. *Water Resour. Res.* **2009**, *45*, W10413. [CrossRef]
33. Zhang, L.; Nan, Z.; Xu, Y.; Li, S. Hydrological impacts of land use change and climate variability in the headwater region of the Heihe River Basin, Northwest China. *PLoS ONE* **2016**, *11*, e0158394. [CrossRef]
34. Ayers, J.R.; Villarini, G.; Schilling, K.; Jones, C. On the statistical attribution of changes in monthly baseflow across the US Midwest. *J. Hydrol.* **2021**, *592*, 125551. [CrossRef]
35. Zhang, J.; Zhang, Y.; Song, J.; Cheng, L.; Paul, P.K.; Gan, R.; Shi, X.; Luo, Z.; Zhao, P. Large-scale baseflow index prediction using hydrological modelling, linear and multilevel regression approaches. *J. Hydrol.* **2020**, *585*, 124780. [CrossRef]
36. Huang, X.-d.; Wang, D.; Han, P.-p.; Wang, W.-c.; Li, Q.-j.; Zhang, X.-l.; Ma, M.-w.; Li, B.-j.; Han, S.-j. Spatial patterns in baseflow mean response time across a watershed in the Loess Plateau: Linkage with land-use types. *For. Sci.* **2020**, *66*, 382–391. [CrossRef]
37. Aboelnour, M.A.; Engel, B.A.; Frisbee, M.D.; Gitau, M.W.; Flanagan, D.C. Impacts of watershed physical properties and land use on baseflow at regional scales. *J. Hydrol. Reg. Stud.* **2021**, *35*, 100810. [CrossRef]
38. Hagedorn, B. Hydrograph separation through multi objective optimization: Revealing the importance of a temporally and spatially constrained baseflow solute source. *J. Hydrol.* **2020**, *590*, 125349. [CrossRef]
39. Arnold, J.G.; Williams, J.R.; Maidment, D.R. Continuous-time water and sediment-routing model for large basins. *J. Hydrol. Eng.* **1995**, *121*, 171–183. [CrossRef]
40. Wei, C.; Dong, X.; Yu, D.; Liu, J.; Reta, G.; Zhao, W.; Kuriqi, A.; Su, B. An alternative to the Grain for Green Program for soil and water conservation in the upper Huaihe River basin, China. *J. Hydrol. Reg. Stud.* **2022**, *43*, 101180. [CrossRef]
41. Bo, H.; Dong, X.; Li, Z.; Hu, X.; Reta, G.; Wei, C.; Su, B. Impacts of climate change and human activities on runoff variation of the intensive phosphate mined Huangbaihe River basin, China. *Water* **2019**, *11*, 2039. [CrossRef]
42. Yu, D.; Dong, X.; Xie, P.; Wei, C.; Liu, J.; Hu, X.; Wang, K.; Xu, S.; Wan, H.; Su, Z. Prioritization of critical source areas for soil and water conservation by using a one-at-a-time removal approach in the upper Huaihe River basin. *Land Degrad. Dev.* **2021**, *32*, 1513–1524. [CrossRef]
43. Wei, C.; Dong, X.; Yu, D.; Zhang, T.; Zhao, W.; Ma, Y.; Su, B. Spatio-temporal variations of rainfall erosivity, correlation of climatic indices and influence on human activities in the Huaihe River Basin, China. *CATENA* **2022**, *217*, 106486. [CrossRef]
44. Peng, S.; Chen, C.; Srinivasan, R.; Zhang, X.; Cai, T.; Fang, X.; Qu, S.; Chen, X.; Li, Q. Evaluating the SWAT Model for Hydrological Modeling in the Xixian Watershed and a Comparison with the XAJ Model. *Water Resour. Manag.* **2011**, *25*, 2595–2612.
45. Aksoy, H.; Kurt, I.; Eris, E. Filtered smoothed minima baseflow separation method. *J. Hydrol.* **2009**, *372*, 94–101. [CrossRef]
46. Cartwright, I.; Gilfedder, B.; Hofmann, H. Contrasts between estimates of baseflow help discern multiple sources of water contributing to rivers. *Hydrol. Earth Syst. Sci.* **2014**, *18*, 15–30. [CrossRef]
47. Fan, Y.; Chen, Y.; Liu, Y.; Li, W. Variation of baseflows in the headstreams of the Tarim River Basin during 1960–2007. *J. Hydrol.* **2013**, *487*, 98–108. [CrossRef]
48. Hagedorn, B.; Meadows, C. Trend Analyses of Baseflow and BFI for Undisturbed Watersheds in Michigan—Constraints from Multi-Objective Optimization. *Water* **2021**, *13*, 564. [CrossRef]
49. Abbaspour, K.C. *SWAT-CUP 2012: SWAT Calibration and Uncertainty Programs–A User Manual*; Eawag: Dübendorf, Switzerland, 2013; Volume 103.
50. Moriasi, D.N.; Arnold, J.G.; Liew, M.W.V.; Bingner, R.L.; Harmel, R.D.; Veith, T.L. Model Evaluation Guidelines for Systematic Quantification of Accuracy in Watershed Simulations. *Trans. ASABE* **2007**, *50*, 885–900. [CrossRef]
51. Staff, S.S. *National Soil Survey Handbook*; US Department of Agriculture: Washington, DC, USA, 1996.
52. Zhang, Z.; Bianchette, T.A.; Meng, C.; Xu, Q.; Jiang, M. Holocene vegetation-hydrology-climate interactions of wetlands on the Heixiazi Island, China. *Sci. Total Environ.* **2020**, *743*, 140777. [CrossRef]
53. Xu, C.; Chen, Y.; Yang, Y.; Hao, X.; Shen, Y. Hydrology and water resources variation and its response to regional climate change in Xinjiang. *J. Geogr. Sci.* **2010**, *20*, 599–612. [CrossRef]
54. Line, D.; White, N. Effects of development on runoff and pollutant export. *Water Environ. Res.* **2007**, *79*, 185–190. [CrossRef] [PubMed]

55. Wine, M.L.; Zou, C.B. Long-term streamflow relations with riparian gallery forest expansion into tallgrass prairie in the Southern Great Plains, USA. *For. Ecol. Manag.* **2012**, *266*, 170–179. [CrossRef]
56. Germer, S.; Neill, C.; Vetter, T.; Chaves, J.; Krusche, A.V.; Elsenbeer, H. Implications of long-term land-use change for the hydrology and solute budgets of small catchments in Amazonia. *J. Hydrol.* **2009**, *364*, 349–363. [CrossRef]
57. Price, K.; Jackson, C.R.; Parker, A.J.; Reitan, T.; Dowd, J.; Cyterski, M. Effects of watershed land use and geomorphology on stream low flows during severe drought conditions in the southern Blue Ridge Mountains, Georgia and North Carolina, United States. *Water Resour. Res.* **2011**, *47*, W02516. [CrossRef]
58. Zhang, R.; Chen, X.; Zhang, Z.; Soulsby, C.; Gao, M. How can streamflow and climate-landscape data be used to estimate baseflow mean response time? *J. Hydrol.* **2018**, *557*, 916–930. [CrossRef]
59. Hellwig, J.; Stahl, K. An assessment of trends and potential future changes in groundwater-baseflow drought based on catchment response times. *Hydrol. Earth Syst. Sci.* **2018**, *22*, 6209–6224. [CrossRef]
60. Dong, J.; Zeng, W.; Wu, L.; Huang, J.; Gaiser, T.; Srivastava, A.K. Enhancing short-term forecasting of daily precipitation using numerical weather prediction bias correcting with XGBoost in different regions of China. *Eng. Appl. Artif. Intell.* **2023**, *117*, 105579. [CrossRef]
61. Rumsey, C.A.; Miller, M.P.; Sexstone, G.A. Relating hydroclimatic change to streamflow, baseflow, and hydrologic partitioning in the Upper Rio Grande Basin, 1980 to 2015. *J. Hydrol.* **2020**, *584*, 124715. [CrossRef]
62. Segura, C.; Noone, D.; Warren, D.; Jones, J.A.; Tenny, J.; Ganio, L.M. Climate, landforms, and geology affect baseflow sources in a mountain catchment. *Water Resour. Res.* **2019**, *55*, 5238–5254. [CrossRef]
63. Peña-Arancibia, J.; Van Dijk, A.; Mulligan, M.; Bruijnzeel, L.A. The role of climatic and terrain attributes in estimating baseflow recession in tropical catchments. *Hydrol. Earth Syst. Sci.* **2010**, *14*, 2193–2205. [CrossRef]
64. Troch, P.A.; Carrillo, G.; Sivapalan, M.; Wagener, T.; Sawicz, K. Climate-vegetation-soil interactions and long-term hydrologic partitioning: Signatures of catchment co-evolution. *Hydrol. Earth Syst. Sci.* **2013**, *17*, 2209–2217. [CrossRef]
65. Nyeko, M. Hydrologic Modelling of Data Scarce Basin with SWAT Model: Capabilities and Limitations. *Water Resour. Manag.* **2015**, *29*, 81–94. [CrossRef]
66. Abbaspour, K.C.; Rouholahnejad, E.; Vaghefi, S.; Srinivasan, R.; Yang, H.; Kløve, B. A continental-scale hydrology and water quality model for Europe: Calibration and uncertainty of a high-resolution large-scale SWAT model. *J. Hydrol.* **2015**, *524*, 733–752. [CrossRef]
67. Aboelnour, M.; Gitau, M.W.; Engel, B.A. A comparison of streamflow and baseflow responses to land-use change and the variation in climate parameters using SWAT. *Water* **2020**, *12*, 191. [CrossRef]
68. Brutsaert, W. Long-term groundwater storage trends estimated from streamflow records: Climatic perspective. *Water Resour. Res.* **2008**, *44*, W02409. [CrossRef]